

II. STATE OF THE ART

Vessel detection has been extensively studied recently, so we have plenty of references on the subject. Datasets like Ships From Google Earth [5] or VHRShips [3] collect remote sensing images to train AI algorithms designed for detecting objects in images like YOLO with really good results ($\sim 90\%$ of accuracy) (Fig. 1). These datasets typically feature images with a small GSD (of around 0.5 meters and at most 1.5 meters). Regarding the detection algorithms, they are computationally expensive compared to classical compression algorithms like JPEG, but the size of the resulting semantic information (the coordinates of the bounding box(es) of the detected vessels) is significantly smaller than compressed images.

Edge computing has recently been applied to LEO satellite constellations to reduce network congestion and latency. In [4], an edge computing framework for EO that optimizes processing load distribution and compression parameters to minimize energy consumption and increase processed information is formulated. [6] proposes a scheduling approach involving observation, relay, and computing satellites to maximize the number of completed observation tasks.

SemCom and GO have been widely studied in terrestrial networks. We refer the reader to [1] for an overview. The case of moving objects in ground has analogies with our tracking problem [7]. In GO designs, the AoI is a common used metric to measure the elapsed time since the generation of the last received update, or, equivalently, the freshness of the information [8]. The age increases linearly in time if there are no updates, and it decreases upon reception of a new update to the time elapsed since such update was generated. The abundance of papers regarding the AoI is overwhelming and there are many proposed variants, being the Peak Age of Information (PAoI) [9] a good option for worst-case optimizations.

III. SYSTEM MODEL

The LEO satellite constellation consists of M circular orbital planes deployed at an altitude h and with a given inclination δ . There are N evenly distributed satellites in each of such orbital planes, i.e., the constellation size is $M \times N$. These four parameters, M , N , h , and δ , are the parameters of interest for the design and dimensioning of the constellation. These have to be selected taking into account performance parameters such as the availability of the service, i.e., the probability of being under the coverage area for a specific service [10], which is also impacted by the latitude. Furthermore, the organization of satellites along the orbital shell (a set of orbital planes displayed at the same altitude) can be of two types: walker star or walker delta. A walker star orbital shell consists of nearly-polar orbits ($\delta \sim 90^\circ$) evenly spaced within 180° (the angle between adjacent orbital planes is $180/N$), while a walker delta orbital shell consists of inclined orbits ($\delta < 60^\circ$) evenly spaced within 360° (the angle between adjacent orbital planes is $360/N$). The constellation is used to capture the images, process them, and send up-to-date information from

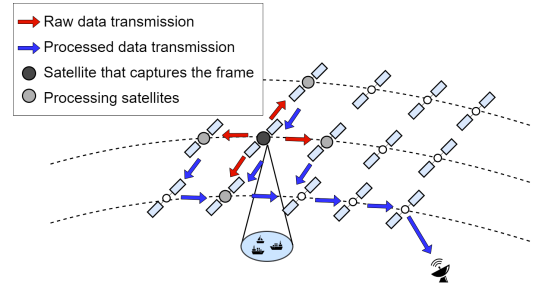


Fig. 2. Sketch of the scenario.

a predetermined area to ground, i.e., to transmit the identified and located vessels. For this, the satellites are equipped with a communication payload and a processing payload. This information is monitored in a predefined GS. The process is as follows (see Fig. 2):

- 1) The area to be monitored is predefined.
- 2) A frame is taken when any of the satellites in the constellation is in a suitable position to capture a quality frame of the area. As this depends on various complex and interrelated factors, it will be considered that a quality photo can be taken up to a specific angle β off-nadir. It will also be assumed that the atmospheric and meteorological conditions are suitable.
- 3) A vessel detection algorithm is applied in a distributed and parallel way by fragmenting the original frame. It is assumed that all satellites in the constellation will have the YOLOv8 [2] vessel detection algorithm on their CPUs, pre-trained with the Ships From Google Earth dataset [5], and will be capable of capturing images with sufficient quality for the algorithm to perform effectively. This algorithm has been selected because, compared to similar ones, it is computationally less expensive. However, the computation load is still considerable, as the amount of information to be processed, so it will be fragmented and equally divided among the satellite that takes the frame and its four neighbors (two in the same orbital plane and two in the adjacent orbital planes). The sections into which the frame has been divided are further divided into images of a specific resolution to be processed (Fig 3).
- 4) The result of the detection is routed to a specific GS. Once processing is complete, the fragmented information consisting of the detected vessels in each fragment is routed to the GS by each satellite participating in the computing, and using the routing algorithm developed in [11]. This derives the path with the shortest propagation distance between two satellites from the paths with the fewest number of hops between them (the minimum hop path region) based on the relationship between satellite phase and inter-satellite link distance.

It should be noted that before taking the next frame, the processing of the last one taken must be fully completed so that the processing load does not accumulate.

To calculate the amount of information sent to the GS, it

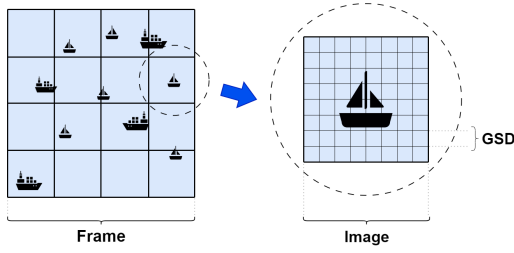


Fig. 3. Example of a frame captured and divided into images of a specific resolution.

must be taken into account the compression factor (ρ) and the portion of images in the captured frame with detected vessels ($\alpha_{vessels}$). The compression factor is given by

$$\rho = \frac{D_{img}}{N_{vessels} D_{bbox}}, \quad (1)$$

where D_{img} is the average size of the image, $N_{vessels}$ the average number of detected vessels per image and D_{bbox} the average size of the bounding boxes. In this way, the amount of information x_g sent to the GS can be calculated as follows:

$$x_g = \frac{x \alpha_{vessels}}{\rho}, \quad (2)$$

where x is the amount of information to process in bits.

Regarding communications, free-space optical (FSO) links will be used for intra-plane Inter-Satellite Link (ISL) and radio frequency (RF) links for inter-plane ISL and the downlink. The transmission rates for the links are obtained as described in [10].

In addition, there are losses both in the communication (packet losses) and in the detection (vessels present in the images but not detected), and they both will affect the timing performance. We will consider a packet loss probability on a link ranging from P_{min} to P_{max} depending on the distance between satellites. This will be given by the following formula:

$$P_{loss} = P_{max} + (P_{min} - P_{max}) \exp\left(-\frac{d}{d_{max} - d_{min}}\right), \quad (3)$$

where d the distance between the two satellites where the links, and d_{max} and d_{min} are maximum and minimum distances between adjacent satellites selected accordingly to the simulated constellations as explained in Section V. For the computation and communication losses the worst-case scenario will be considered. In communications, losing one packet means that the whole frame is lost. Likewise, the losses due to the detection algorithm will be determined by the recall, which relates the number of detected vessels to the actual number of vessels, obtained when testing the algorithm with the test dataset:

$$\text{Recall} = \frac{\text{Number of detected vessels}}{\text{Actual number of vessels}}. \quad (4)$$

IV. CONSTELLATION DESIGN AND TIMING METRICS

A. Constellation design

There are three elements in the system model related to the constellation design. The first one is to decide the value

of some features of the constellation that make feasible to capture images with sufficient quality to perform the vessel detection process. Due to its homogeneity, the images VHRShips dataset, with a GSD of 0.43 m/pixel, has been taken as reference. Moreover, the parameters of the satellite WorldView-3 [12] are suitable to capture images comparable to those in the selected dataset, and therefore has been selected as a reference for the study. The altitude is approximately 600 km. The second step is to decide if the constellation consist of a walker star or a walker delta orbital shell. The criterion here is to cover the largest possible area, but also to ensure that there are the maximum number of satellites in areas of interest, i.e., most of the globe is covered most of the time. Taking into account that the vast majority of vessels located outside of the polar regions [13], we choose a walker delta orbital shell with a sufficient number of satellites in regions of interest. Finally, the density of the constellation must be selected, i.e., the number of orbital planes M and satellites per orbital plane N , for which we aim at ensuring that the average time between capturing one frame and the next one is below a predetermined threshold. These values will be obtained through simulations relying on the coverage probability (P_m) and the AoI as defined next.

B. Timing metrics

Both communication and processing times contribute to the AoI. The frame acquisition time is negligible. For the processing times, the execution times of the algorithm were measured on a personal computer, and these were converted into CPU cycles per bit. From a set of these measurements, a gamma function can be derived to randomize the complexity of the algorithm within a realistic range of values. Thus, given the computational capacity of the satellites (in terms of the number of cores and CPU clock frequency), the processing times can be calculated. Processing times are calculated as:

$$T_{proc} = \frac{xC}{N_{cores} f_{CPU}}, \quad (5)$$

where C is the complexity of the algorithm in CPU cycles per bit, N_{cores} the number of cores of the CPU and f_{CPU} the CPU frequency. Regarding communication, transmission and propagation times, they will be calculated from the satellite taking the frame to its neighbors, plus the transmission and propagation times from the processing-satellites to the GS. For the transmission this is written as the sum over the links l , i.e.,

$$T_{trixon} = \sum_l \frac{D_l}{R_l}, \quad (6)$$

where D_l is the number of bits to transmit through a given link l and R_l the bit rate of such link. And for the propagation:

$$T_{prop} = \frac{\sum_l d_l}{c}, \quad (7)$$

where d_l is the distance between two nodes of the path obtained from the routing algorithm [11], which determines the path with the minimum propagation distance between two

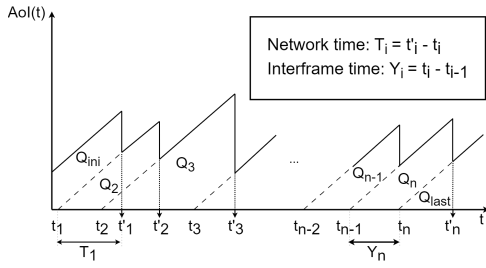


Fig. 4. Evolution of the AoI.

satellites among those with the minimum number of hops; and c the speed of light.

The AoI is reformulated to consider the instant at which the frames are captured and at which the information of the mapped area reaches the GS. Mathematically, this is expressed as follows. Fig. 4 shows the time evolution of the AoI. It is assumed that the system is first observed at $t = 0$ and index i represents the number of the frame. A frame i is captured at $t = t_i$ and its semantic information is fully received at the GS at $t = t'_i$. As the processing task is distributed in parallel among multiple satellites and the resulting data is routed through different paths to the destination, there will be several timestamps representing the reception of semantic information in the GS, of which the largest one will be considered, representing the time in which all processed information is available at the GS and therefore the remote monitor has the full information of the mapped area. Assuming the processing is distributed among n satellites:

$$t'_i = \max \left\{ t_i^{(1)}, t_i^{(2)}, \dots, t_i^{(n-1)}, t_i^{(n)} \right\}. \quad (8)$$

T_i is defined as the total network time of the system (communication + processing times); and Y_i as the interframe time $T_i = t'_i - t_i$, the time between the capture of the frames whose semantic information is subsequently received $Y_i = t_i - t_{i-1}$.

The average AoI can be calculated as follows:

$$\text{AoI}_{avg} = \frac{1}{\tau} \left(Q_{ini} + Q_{last} + \sum_{i=2}^{N(\tau)} Q_i \right); \quad (9)$$

where τ is the total observation time and $N(\tau)$ the the number of arrivals by that time. As can be seen in Fig. 4, Q_i for $1 < i$ are trapezoids whose areas can be calculated as:

$$Q_i = \frac{1}{2} (T_i + Y_i)^2 - \frac{1}{2} T_i^2 = Y_i T_i + \frac{Y_i^2}{2}. \quad (10)$$

Likewise, assuming that the system is observed for the first time at $t = 0$, the average PAoI can be calculated as:

$$\text{PAoI}_{avg} = \frac{1}{N(\tau)} \left(t'_1 + \sum_{i=2}^{N(\tau)} (t'_i - t_{i-1}) \right). \quad (11)$$

V. SIMULATION AND RESULTS

The first orbital shell of Starlink has been used as the reference constellation because its altitude (~ 550 km) is suitable for

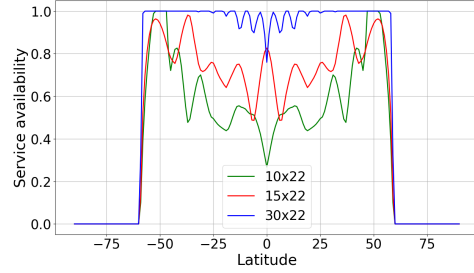


Fig. 5. Service availability taking a quality frame for vessel detection. Starlink-like topology with $M = 10, 15, 30$, and $N = 22$.

obtaining quality images and the orbital shell is of the walker delta type ($\delta = 53^\circ$). In order to obtain the density of the constellation which allows to have an average PAoI value below a certain threshold, two series of simulations will be carried out. The first one will be conducted by fixing N and varying M to determine the number of orbital planes and, once it has been determined, the second one will be conducted by fixing M and varying N to determine the number of satellites per orbital plane. Regarding the packet loss probability, values between $P_{min} = 0.001$ and $P_{max} = 0.1$ have been considered, as they can be considered typical values [14], and d_{max} and d_{min} are the maximum and minimum distances between satellites for the constellations considered for the simulations, respectively. For the computation losses, a recall of 0.9 is assumed. It will be considered that the information is updated with sufficient frequency if the average PAoI is less than 60 seconds.

The simulations aim to calculate the AoI over a period of Earth rotation to obtain the average AoI and PAoI for a specific coordinate to be monitored. As the probability of taking a quality frame depends on the coordinate to be monitored (see Fig. 5) a series of Monte Carlo simulations will be conducted by randomizing it, ultimately obtaining the average values. To ensure that the area to be monitored is in a water-covered region, the coordinates prone to be selected have been restricted to those shown in Fig. 6 and the GS to which the resulting information will be sent will be located in Los Angeles (latitude 34.05° , longitude -118.24°). It will be assumed that a certain amount of vessels are always in the area to be monitored and that the area covered by a frame is 162.16 km^2 . Other relevant parameters for the simulation are: $f_{CPU} = 1.8 \text{ kHz}$, $N_{cores} = 8$, $\beta = 50^\circ$, $D_{img} = 391.43 \text{ kB}$, $GSD = 0.43 \text{ m/pixel}$, an image resolution of 720×1280 pixels, $D_{bbox} = 67.2 \text{ bits}$, an average C of $374.2 \text{ CPU cycles per bit}$, $\rho = 23299.4$, and $\alpha_{vessels} = 0.2$.

Fig. 7 shows the results of the first sweep, keeping N fixed, displaying the average AoI and PAoI, along with the probability P_m of covering the specific monitored area over a rotation period of the Earth for different number of orbital planes. It concludes that 20 orbital planes ensure an average PAoI below the established threshold with $P_m \sim 100\%$. Thus, the results of the second sweep, with $M = 20$, are shown in Fig. 8, also displaying the average AoI and PAoI along with P_m . According to them, it is possible to achieve an average

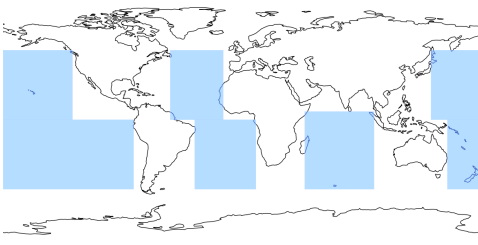


Fig. 6. Coordinates prone to be selected for water-covered regions.

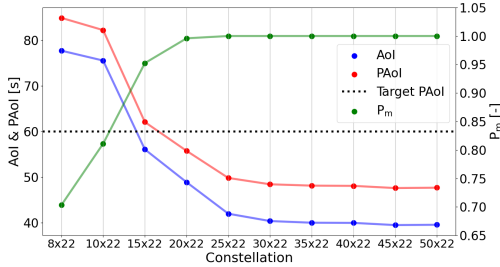


Fig. 7. Average AoI and PAoI and probability of coverage of the monitored area (P_m) for Starlink-like topology with $N = 22$ and varying M .

PAoI below the threshold with $N = 20$. P_m does not vary significantly.

Once the constellation size is determined, the effect of varying the number of processing satellites is assessed. Fig. 9 shows the average AoI and PAoI with different numbers of processing satellites. Without losses, more processing satellites reduce both AoI and PAoI. However, considering losses, five processing satellites (the one taking the frame and its four neighbors) is adequate for the proposed scenario. Fewer processing satellites fail to meet the target PAoI, and more of them do not improve results and may worsen them due to increased packet loss probability.

Thus, five cooperating satellites in a walker delta orbital shell with $h = 550$ km, $\delta = 53^\circ$ and a size of 20×20 can accomplish the task while keeping the PAoI below 60 seconds. Furthermore, the amount of information to be transmitted is reduced from 2.98 Gb (the average frame size) to 127.81 Kb (the total size of the bounding boxes for the simulation parameters), i.e., a size reduction of 99.996%.

VI. CONCLUSIONS

In this paper, we investigate the potential of a LEO satellite constellation for near real-time vessel detection in a predefined geographical area, leveraging the distributed computation and communication capabilities of the spacecrafts. We apply a real data set and state-of-the-art YOLOv8 algorithm for the detection, and dimension the constellation for the best tradeoff between freshness of the information at the receiver and accuracy in the accomplishment of the task. The presented model can serve as a complement to Automatic Identification Systems (AIS) for vessel tracking [13]. Future work will generalize the model by considering the queries from ground (i.e., a closed-loop communication), the impact of atmospheric turbulences, and more comprehensive simulations.

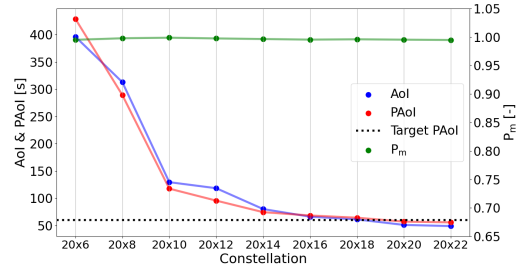


Fig. 8. Average AoI and PAoI and probability of coverage of the monitored area (P_m) for Starlink-like topology with $M = 20$ and varying N .

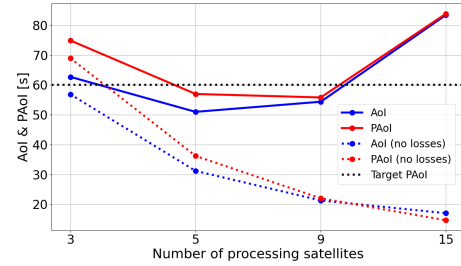


Fig. 9. Average AoI and PAoI for a Starlink-like topology with $M = 20$ and $N = 20$ varying the number of processing satellites.

REFERENCES

- [1] D. Gündüz *et al.*, “Beyond transmitting bits: Context, semantics, and task-oriented communications,” *IEEE Journal on Selected Areas in Communications*, vol. 41, no. 1, pp. 5–41, 2023.
- [2] G. Jocher, A. Chaurasia, and J. Qiu, “Ultralytics yolov8,” 2023. [Online]. Available: <https://github.com/ultralytics/ultralytics>
- [3] S. Kızılkaya *et al.*, “Vhrships: An extensive benchmark dataset for scalable deep learning-based ship detection applications,” *ISPRS International Journal of Geo-Information*, vol. 11, no. 8, 2022.
- [4] I. Leyva-Mayorga *et al.*, “Satellite edge computing for real-time and very-high resolution earth observation,” *IEEE Transactions on Communications*, vol. 71, no. 10, p. 6180–6194, Oct. 2023.
- [5] K. Stavrakakis, “Ships-google-earth dataset,” <https://universe.roboflow.com/k--stavrakakis/ships-google-earth>, May 2022, visited 2024-03-18.
- [6] B. Zhu, S. Lin, Y. Zhu, and X. Wang, “Collaborative hyperspectral image processing using satellite edge computing,” *IEEE Transactions on Mobile Computing*, vol. 23, no. 3, pp. 2241–2253, 2024.
- [7] N. Pappas and M. Kountouris, “Goal-oriented communication for real-time tracking in autonomous systems,” in *2021 IEEE International Conference on Autonomous Systems (ICAS)*, 2021, pp. 1–5.
- [8] A. Kosta, N. Pappas, and V. Angelakis, “Age of information: A new concept, metric, and tool,” *Foundations and Trends® in Networking*, vol. 12, no. 3, pp. 162–259, 2017.
- [9] F. Chiariotti, B. Soret, and P. Popovski, “Latency and peak age of information in non-preemptive multipath communications,” *IEEE Transactions on Communications*, vol. 70, no. 8, pp. 5336–5352, 2022.
- [10] E. Lagunas, S. Chatzinotas, K. An, and B. F. Beidas, Eds., *Non-Geostationary Satellite Communications Systems*. Institution of Engineering and Technology, Dec. 2022. [Online]. Available: <http://dx.doi.org/10.1049/PBTE105E>
- [11] Q. Chen, L. Yang, Y. Zhao, Y. Wang, H. Zhou, and X. Chen, “Shorted path in leo satellite constellation networks: An explicit analytic approach,” *IEEE Journal on Selected Areas in Communications*, 12 2023.
- [12] DigitalGlobe, “Worldview-3 datasheet,” 2017.
- [13] “Marine traffic: Global ship tracking intelligence.” [Online]. Available: <https://www.marinetraffic.com>
- [14] I. Akyildiz, E. Ekici, and M. Bender, “Mlsr: A novel routing algorithm for multilayered satellite ip networks. *ieee/acm transactions on networking*,” *IEEE/ACM Trans. Netw.*, vol. 10, pp. 411–424, 06 2002.